SIMULATIONS OF 2-D LAMINAR FLOW PAST A BLUFF BODY IN A CLOSED CHANNEL WITH A TRULY INCOMPRESSIBLE SPH

E.-S. Lee(1), C. Moulinec(2), D. Violeau(3), D. Laurence(4), P. Stansby(5)

[1]School of Mechanical, Aerospace and Civil Engineering, The University of Manchester, PO Box 88, Manchester M60 1QD, UK,
phone: +44 161 306 2615; fax :+44 161 306 3723; e-mail: e.lee-2@postgrad.manchester.ac.uk

[2] Laboratoire National d'Hydraulique et Environnement (LNHE), EDF R&D, 6 quai Watier, BP 49, 78400 Chatou, France
phone: +33 1 30 87 83 98; fax :+33 1 30 87 80 86; e-mail: chmoulinec@yahoo.com

[3] Laboratoire National d'Hydraulique et Environnement (LNHE), EDF R&D, 6 quai Watier, BP 49, 78400 Chatou, France
phone: +33 1 30 87 78 31; fax :+33 1 30 87 80 86; e-mail: damien.violeau@edf.fr

[4]School of Mechanical, Aerospace and Civil Engineering, The University of Manchester, PO Box 88, Manchester M60 1QD, UK,
phone: +44 161 306 3704; fax :+44 161 306 3723; e-mail: dominique.laurence@manchester.ac.uk

[5]School of Mechanical, Aerospace and Civil Engineering, The University of Manchester, PO Box 88, Manchester M60 1QD, UK,
phone: +44 161 306 4598; fax :+44 161 306 4646; e-mail: p.k.stansby@manchester.ac.uk

ABSTRACT

A truly incompressible SPH (ISPH) has been developed to circumvent some drawbacks found in weakly compressible SPH (WCSPH) such as large pressure fluctuations due to the error in density, and very expensive computation time due to the required CFL condition. One of the main differences between WCSPH and ISPH is the pressure solver; the former one is based on the equation of state for water and the latter one solves a pressure Poisson equation. The pressure Poisson equation is solved in this work by Bi-CGSTAB method. 2-D laminar flows (Re_D = 20 and 100) past a square and a circular cylinder in a confined closed channel are simulated to investigate the ability of the ISPH method to handle flows past obstacles. ISPH results here are compared to data obtained by an Eulerian software (STAR-CD V4) with a satisfactory agreement.

Keywords: SPH, truly incompressible, 2-D bluff body, square cylinder, circular cylinder, laminar flow, vortex shedding

1 INTRODUCTION

The SPH (Smoothed Particle Hydrodynamics) method is a fully Lagrangian (gridless) numerical method invented to simulate astrophysical problems at the end of the 70's (Monaghan 1992). This method has then been successfully applied to other fields such as fluid and solid mechanics. One of the distinct features of this method is that it does not require any mesh to cover the fluid domain. Instead, this fluid domain is represented by a set of macroscopic fluid particles which interact and move according to forces derived from the equations of motion. This approach is very attractive to model complex flows, as for instance free surface flows.

The traditional SPH method solves weakly compressible (WCSPH) flows in the sense that relative density variations range within 1% (Monaghan 1992). Although this method is robust and very easy to program when implemented in an explicit way, it shows some drawbacks, as for instance pressure fluctuations and very long CPU time. A truly incompressible SPH

(ISPH) has been developed to circumvent these problems. The main difference between WCSPH and ISPH is the way of obtaining pressure. The former uses a state equation for water and the latter solves a pressure Poisson equation, which avoids the large pressure fluctuations observed with the state equation. In addition, maximum fluid velocity is used in CFL condition for ISPH while a numerical speed of sound (10 times higher than maximum fluid velocity) is used for WCSPH, which makes the time step smaller.

In the following, the ISPH method is briefly introduced. Since the development of ISPH is still an ongoing process, academical cases, such as 2-D laminar flow past a square and a circular cylinder, are chosen to investigate ISPH behaviour by comparing it with an Eulerian code (STAR-CD V4) one based on a finite volume approach. Drag coefficient and recirculation length from both methods are compared for all cases. For the case of $\mathrm{Re}_D = 100$, Strouhal number is given. The influence of fluid discretisation is also studied in the case of a circular cylinder at $\mathrm{Re}_D = 20$.

2 A TRULY INCOMPRESSIBLE SPH METHOD

In SPH, a particle represents a macroscopic volume of fluid. Each fluid particle, for example particle a, carries information of a mass m_a, a density ρ_a, a pressure p_a, a velocity $\mathbf{u}_a$, a position $\mathbf{r}_a$ and other quantities. The mass and density in the present work are constant through the simulations, however, pressure, velocity, position and other physical quantities are updated every time step. Any quantity A attached to a particle a at a position $\mathbf{r}_a$ is written as:

$$A(\mathbf{r}_a) \approx \sum_b \frac{m_b}{\rho_b} A_b w_h(r_{ab}) \tag{1}$$

where the subscript b is used to describe any particle in the neighbourhood of particle a. The distance from a to b is $r_{ab} = (|\mathbf{r}_a - \mathbf{r}_b|)$, A_b denotes the value of any quantity A at $\mathbf{r}_b$. According to Morris *et al*. (1997), a kernel function w_h can be written in a general manner as:

$$w_h(r_{ab}) = \frac{1}{h^\sigma} f\left(\frac{r_{ab}}{h}\right) \tag{2}$$

where σ is the dimension of the system and the smoothing length h is proportional to the particle distance, which plays a role similar to the mesh size in Eulerian codes. As shown in Eq. (1), the kernel varies with the distance r_{ab} between particles only.

2.1 ISPH ALGORITHM

Lagrangian Navier-Stokes equations for incompressible laminar flow read:

$$\nabla \cdot \mathbf{u} = 0 \tag{3}$$

$$\frac{d\mathbf{u}}{dt} = -\frac{1}{\rho}\nabla p + \nu \nabla^2(\mathbf{u}) + \mathbf{F}^e \tag{4}$$

where ρ is the density, $\mathbf{u}$ is the velocity vector, t the time, p the pressure, ν the kinematic viscosity and $\mathbf{F}^e$ an external force such as a driving force, for instance. The momentum equation (4) is split into two parts by using the classical projection method (Chorin 1968) to solve the velocity-pressure coupling problem; the first being the prediction step based on viscous and external forces:

$$\frac{\mathbf{u}^* - \mathbf{u}^n}{\Delta t} = \nu \nabla^2(\mathbf{u}^n) + \mathbf{F}^e \tag{5}$$

and the second the correction step based on pressure force:

$$\frac{\mathbf{u}^{n+1} - \mathbf{u}^*}{\Delta t} = -\frac{1}{\rho}\nabla p^{n+1} \tag{6}$$

where Δt is the numerical time step, $\mathbf{u}^*$ is an auxiliary velocity and the superscripts n and n+1 indicate previous and present time steps. The auxiliary velocity field $\mathbf{u}^*$ is usually not divergence free and continuity is imposed upon $\mathbf{u}^{n+1}$. Hence, the auxiliary velocity is projected on the divergence-free space by taking the divergence of Eq. (6), which leads to:

$$\nabla^2 p^{n+1} = \frac{\rho}{\Delta t} \nabla \cdot \mathbf{u}^* \tag{7}$$

where ∇^2 is the Laplacian operator. The pressure is obtained form the Eq. (7) through the Bi-CGSTAB method (Van Der Vorst 1992). Then, the auxiliary velocity is corrected by the computed pressure gradient to give $\mathbf{u}^{n+1}$ as:

$$\mathbf{u}^{n+1} = \mathbf{u}^* - \left(\frac{1}{\rho} \nabla p^{n+1} \right) \Delta t \tag{8}$$

Finally, particles move only with this corrected velocity by the following relation:

$$\mathbf{r}^{n+1} = \mathbf{r}^n + \mathbf{u}^{n+1} \Delta t \tag{9}$$

2.2 EQUATIONS IN SPH FORMULATION

There are various forms of expressing gradient and divergence operator in SPH (Monaghan 1992). For example, the pressure gradient term can be approximated in SPH formalism as:

$$\nabla p_a \approx \rho_a \sum_b m_b \left(\frac{p_b}{\rho_b^2} + \frac{p_a}{\rho_a^2} \right) \nabla_a w_h(r_{ab}) \tag{10}$$

where $\nabla_a w_h(r_{ab})$ is the kernel gradient, which is taken as centred on the position of particle a. The velocity divergence can read:

$$\nabla \cdot \mathbf{u}_a \approx -\frac{1}{\rho_a} \sum_b m_b \mathbf{u}_{ab} \cdot \nabla_a w_h(r_{ab}) \tag{11}$$

where $\mathbf{u}_{ab} = \mathbf{u}_a - \mathbf{u}_a$. The viscous term is not directly built as a divergence of a gradient, but as a combination of finite difference approach and SPH formalism. We use here the formulation proposed by Monaghan (1992):

$$\nu \nabla^2 \mathbf{u}_a \approx \sum_b m_b \left(\frac{16\nu}{\rho_a + \rho_b} \frac{\mathbf{u}_{ab} \cdot \mathbf{r}_{ab}}{r_{ab}^2 + \eta^2} \right) \cdot \nabla_a w_h(r_{ab}) \tag{12}$$

where $\mathbf{r}_{ab} = \mathbf{r}_a - \mathbf{r}_b$ and $\eta^2 = 0.01h^2$ is a parameter to avoid a zero denominator. The Laplacian operator is then expressed in a similar manner as the viscous term as

$$\nabla^2 p_a \approx \frac{2}{\rho_a} \sum_b m_b \frac{p_{ab} \mathbf{r}_{ab} \cdot \nabla_a w_h(r_{ab})}{r_{ab}^2 + \eta^2} \tag{13}$$

where $p_{ab} = p_a - p_b$. Some other ways to write Laplacian operators can be found in Cummins *et al*. (1999) or Shao *et al*. (2003).

The time step Δt is chosen as the minimum of three conditions, the CFL condition, the mass condition and the viscous force conditions, such that:

$$\Delta t = \min \left(0.4 \frac{h}{u_{\max}}, 0.25 \min_a \sqrt{\frac{h}{|\mathbf{f}_a|}}, 0.125 \min_a \frac{h^2}{\nu_a} \right) \tag{14}$$

where $|\mathbf{f}_a|$ is the force per unit mass, equivalent to the magnitude of particle acceleration.

2.3 BOUNDARY CONDITIONS

Any quantity for particle a in SPH is obtained from the contribution of its neighbouring particles which are located in a compact disk. When the fluid particles are located near a solid boundary, the compact disk is no longer a "physical disk", but degenerates in a truncated disk.

Practically, it means that the information in *a* suffers from the lack of neighbouring particles. There are several techniques to circumvent this problem such as mirror particles (Cummins *et al*. 1999), repulsive forces (Cleary *et al*. 1999) and dummy particles (Shao *et al*. 2003). In this work, the dummy particles technique is chosen for simplicity reason. The wall therefore consists of one layer of edge particles, which materialise the wall, and four layers of dummy particles. The characteristic of these particles are identical as the fluid particles except that they anchor at their initial position through the simulation. While no-slip boundary conditions are imposed at a wall, the pressure for the edge particles is obtained from the Eq. (7) and then allocated to the dummy particles in their normal direction.

3 A LAMINAR FLOW AT $Re_D = 20$

3.1 SYSTEM MODELLING AND SIMULATION CONDITIONS

The geometry is based on Kim *et al*. (2004) one. As shown in Fig. 1, a cylinder of diameter *D* is located at equal distance from two parallel flat plates separated from each other by a distance of 5*D*, the upstream end of the domain being set at a distance of *3D* from the cylinder centre and the downstream end at *LD* of *28D*. Such a long channel is used to ensure that the flow past the cylinder re-develops when periodic boundary condition are applied at both ends of the channel.

All parameters are normalised by the mean bulk velocity at the inlet U_0 and the density is set to unity. The Reynolds number based on the diameter reads $Re_D = U_0D/\nu$ is 20. The flow is driven by a force relative to the prescribed mean bulk velocity at the inlet, which ensures constant flow rate and Reynolds number. All simulations are carried out on an Intel Pentium D CPU 3.00GHz with 2.0G RAM.

Two types of bluff bodies are considered: a square cylinder and a circular one. Concerning the SPH simulations, a total of 18,938 particles (15,608 fluid particles, 682 edge particles and 2,648 dummy particles) is used for the square cylinder simulation and of 18,942 particles (15,632 fluid particles, 662 edge particles and 2,648 dummy particles) for the circular one. The Lagrangian simulations are performed in an unsteady way with an explicit Euler scheme. Initially, the particles are regularly distributed with a distance of 0.1*D* from each other.

The mesh in STAR-CD V4 for the square cylinder is made of 39,392 cells, the height of the first cell being 0.005*D* while 41,472 cells are generated for the circular cylinder and the height of the first cell is 0.024*D*. The Eulerian simulations are performed in a steady way, as no vortex shedding occurs. A stopping criterion is required to stop the calculation. It is set to 1.E-13 is used for both square and circular cylinder calculations.

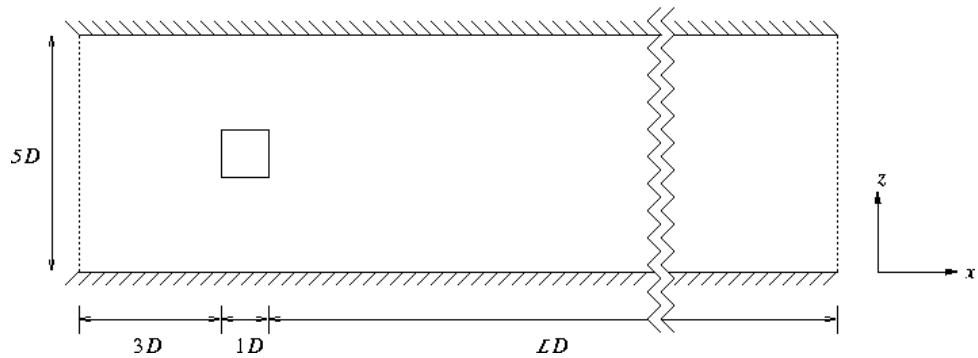

Figure 1. Geometry of the 2-D bluff body in the case of square cylinder case.

3.2 RESULTS ON A SQUARE CYLINDER

ISPH results are time-averaged for postprocessing reasons and then compared with converged STAR-CD V4 ones in terms of normalised axial velocity as shown in Fig. 2. Velocity vectors are depicted in Fig. 3 to compare the recirculation length between ISPH and STAR-CD V4.

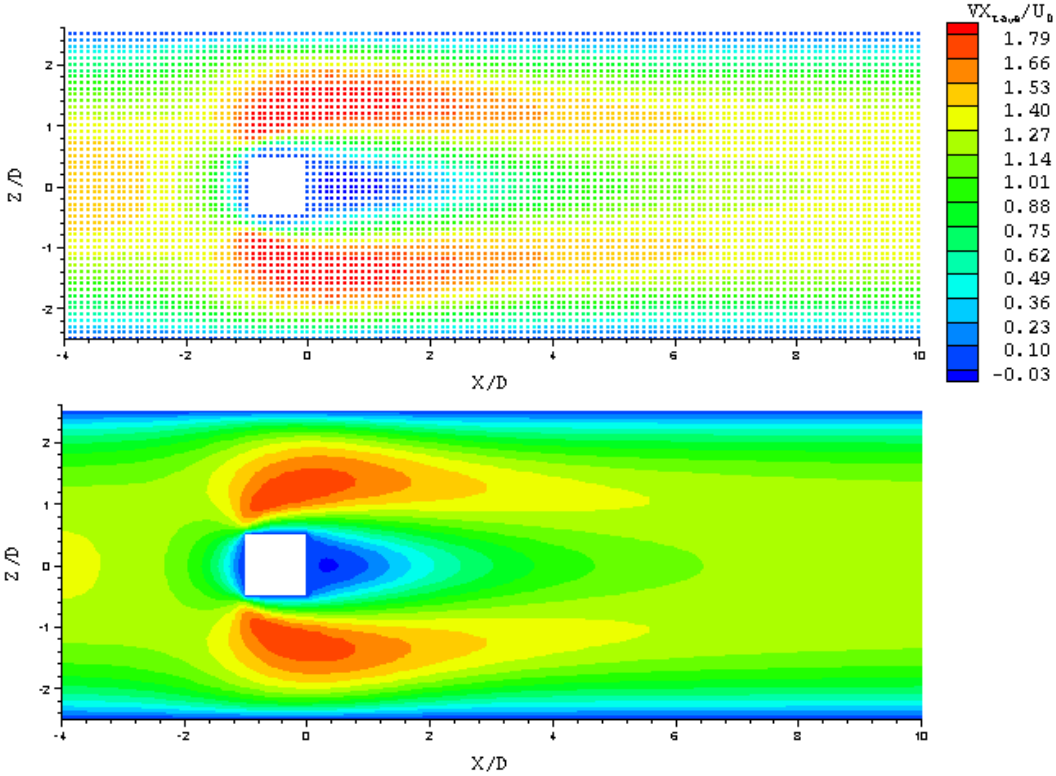

Figure 2. Normalised axial velocity around the square cylinder at $Re_D = 20$. Time-averaged ISPH results against converged STAR-CD V4 ones (top: ISPH, bottom: STAR-CD V4).

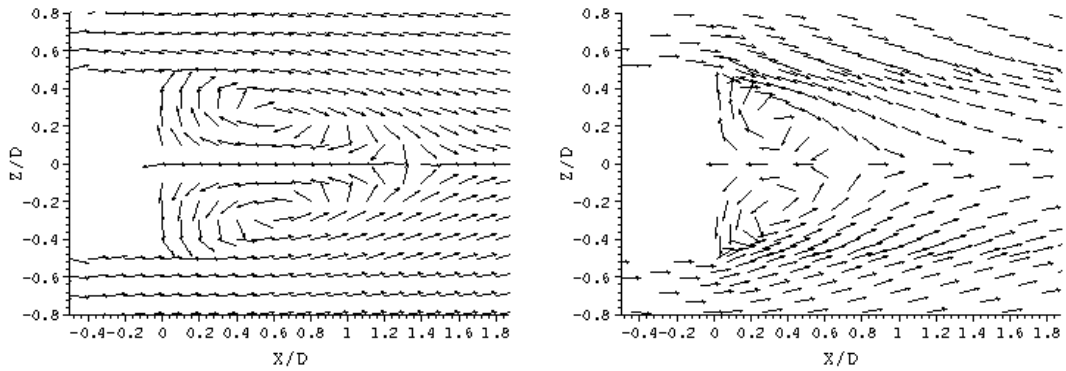

Figure 3. Distributions of uniform velocity vectors behind of the square cylinder for $Re_D = 20$. Time-averaged ISPH results against converged STAR-CD V4 ones (left: ISPH, right: STAR-CD V4).

Dhiman *et al*. (2005) investigated the effect of Reynolds number and of the ratio between the channel height and the square cylinder diameter. According to this paper, the dimensionless recirculation length is in a range of 0.67 and 0.88. The recirculation length from the STAR-CD V4 is reasonably good while ISPH simulation overestimates it.

The drag and lift coefficients are respectively 3.26 and 0.00 with the ISPH algorithm and 4.23 and 0.00 with the Eulerian code. ISPH requires 20 hours to reach the physical time of 520*s* whereas the Eulerian approach 1 hour to reach the stopping criterion.

3.3 RESULTS ON A CIRCULAR CYLINDER

ISPH results are again time-averaged and then compared with converged STAR-CD V4 ones in terms of normalised axial velocity as shown in Fig. 4. Then, velocity vectors are plotted in Fig. 5 to compare the recirculation length between both Lagrangian and Eulerian approaches. While the former shows no big influence depending on the shape of bluff body, the dimensionless recirculation length being 1.28, the latter shows a short recirculation length of 0.44. The drag and lift coefficients are respectively 3.99 and 0.05 for the former and 3.11 and 0.00 for the latter.

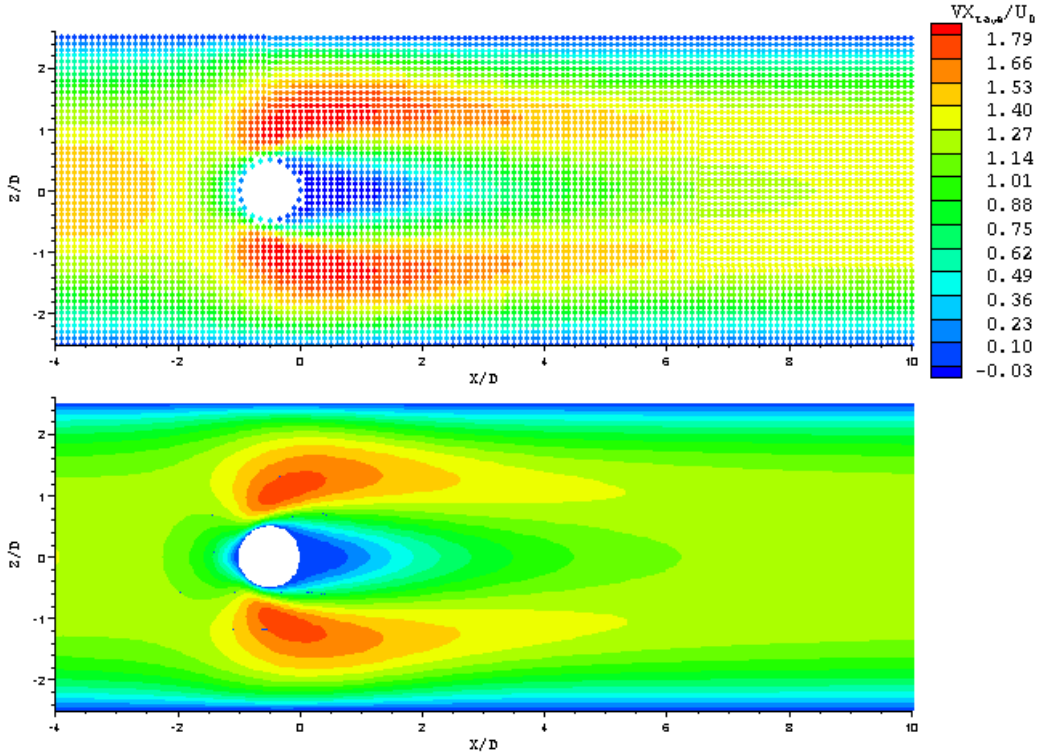

Figure 4. Normalised axial velocity around the circular cylinder $Re_D = 20$. Time-averaged ISPH results against converged ones (top: ISPH, bottom: STAR-CD V4).

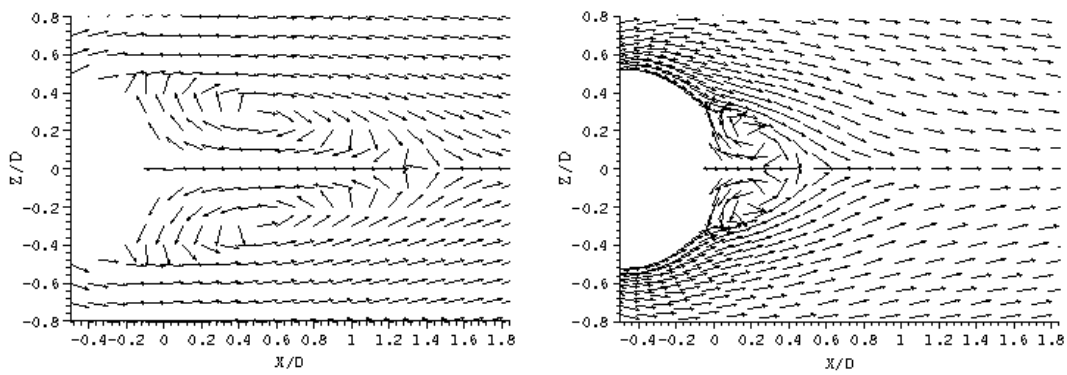

Figure 5. Distributions of uniform velocity vectors behind of the circular cylinder for $Re_D = 20$. Time-averaged ISPH results against converged STAR-CD V4 ones (left: ISPH, right: STAR-CD V4).

4 A LAMINAR FLOW AT $Re_D = 100$

4.1 SYSTEM MODELLING AND SIMULATION CONDITIONS

At this higher Reynolds number, the length of the domain is set to 20 times the inlet height to ensure the flow redevelopment past the cylinder, despite the expected vortex shedding. The length of the channel *LD* after the cylinder in Fig. 1 is set to 98*D*. In this section, the results are presented for the square cylinder only.

A total of 60,238 particles (49,908 fluid particles, 2,082 edge particles and 8,248 dummy particles) is used in the Lagrangian approach. The mesh in the Eulerian one is made of 63,180 cells, the height of the first cell being 0.02*D*. As the flow follows a unsteady motion, a second order accurate scheme is used to perform the time integration.

The Reynolds number based on the diameter Re_D is increased to 100 and periodic boundary conditions are applied in the streamwise direction for both configurations.

4.2 RESULTS ON A SQUARE CYLINDER

Snapshots of axial velocity from both methods are shown in Fig. 7 at the same physical time of $t = 520s$. It shows the front part of the channel from the inlet only.

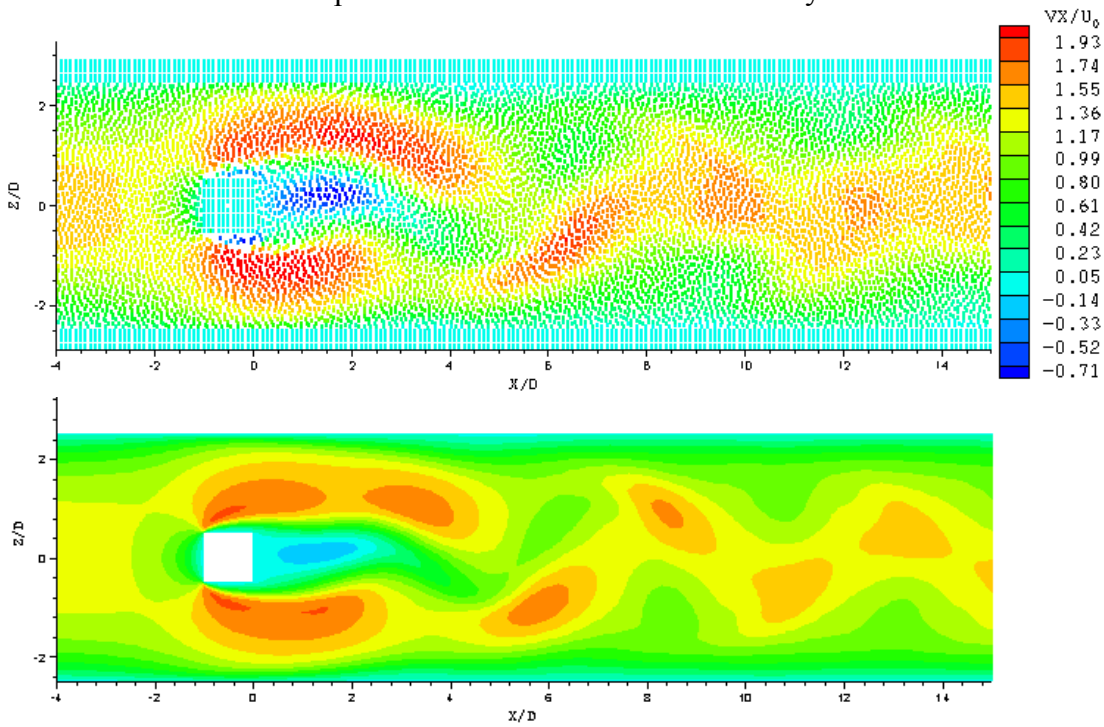

Figure 7. Normalised axial velocity around the square cylinder at $Re_D = 100$ at $t = 520s$ (top: ISPH, bottom: STAR-CD V4).

Both methods give the same vortex shedding. At this point, the Strouhal number fD/U_0, where f is frequency, D the diameter of the cylinder and U_0 is the mean flow velocity, is calculated. The Lagrangian method gives a period f of 1.95s and the Eulerian ones of 2s with $D = 1$m and $U_0 = 1\text{m}\cdot\text{s}^{-1}$, thus $St = 0.51$ for the former and $St = 0.50$ for the latter. The results are now time-averaged to examine the recirculation length and averaged velocity vectors are plotted in Fig. 8. The dimensionless recirculation length given by ISPH is 1.8 and 2.1 by the Eulerian code.

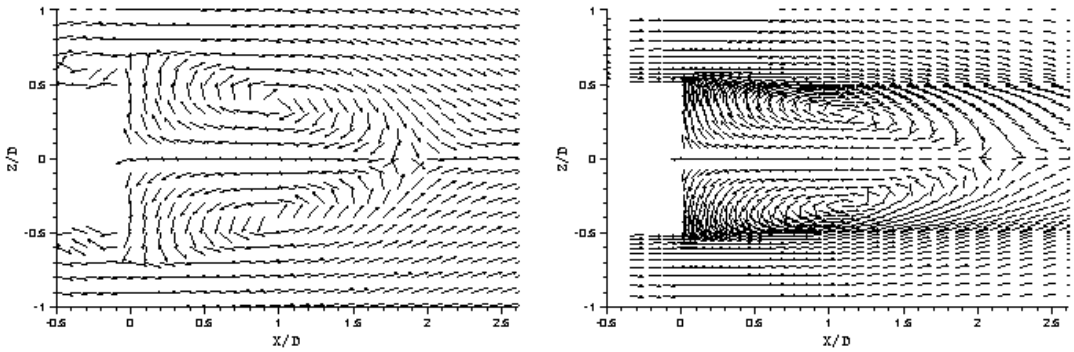

Figure 8. Distributions of uniform time-averaged velocity vectors past a square cylinder for $Re_D = 100$ with ISPH results on the left and STAR-CD V4 ones the right.

The drag coefficient given by ISPH is 3.21 while it is 2.72 in the finite volume simulation. The CPU time in ISPH takes 4 days to have the physical time of 520*s* and 10 hours for STAR-CD V4.

5 INFLUENCE OF THE INITIAL PARTICLE DISTRIBUTION AT $Re_D = 20$ WITH ISPH

All simulation conditions are identical to the circular cylinder case with $Re_D = 20$ (see Section 3.3), except that the initial particle distance is reduced by half to give 0.05*D*. This leads to a new total of 69,738 particles (63,078 fluid particles, 1,332 edge particles and 5,328 dummy particles).

As expected, the flow pattern is similar to what is shown in Section 3.3, hence, only time-averaged velocity vectors behind the cylinder are shown to investigate the influence of the initial particle distribution on the dimensionless recirculation length. This finer one reduces the recirculation length from 1.28 to 1.0. The CPU time in this finer case is 8 days to reach the physical time of 520*s*.

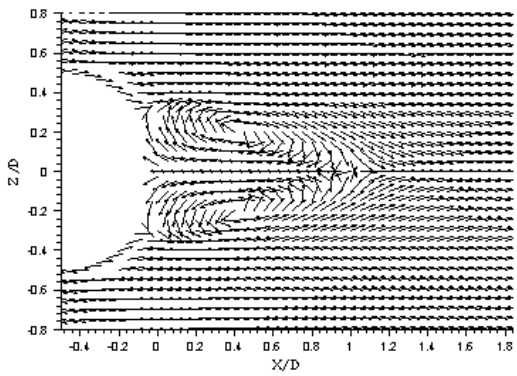

Figure 9. Distributions of uniform velocity vectors behind a circular cylinder at $Re_D = 20$ with a finer initial particle distribution. Time-averaged ISPH results (initial particle distance $dr = 0.05D$).

6 CONCLUSIONS

Drag and lift coefficients and dimensionless recirculation length obtained by ISPH and the Eulerian method are summarised in Table 1. At Re_D=20, the recirculation length obtained by ISPH simulations seems to be not strongly affected by the shape of the bluff body on the contrary to what occurs in Eulerian simulations. In comparison to the latter, the ISPH model

slightly overestimated the drag coefficients. At Re_D = 100, both methods show the same vortex shedding at the physical time of t = 520s.

	Re_D=20				Re_D=100	
	Circular cylinder		Square cylinder		Square cylinder	
	ISPH	STAR-CD	ISPH	STAR-CD	ISPH	STAR-CD
Drag coefficient	3.99	3.11	3.26	4.23	3.21	2.72
Lift coefficient	0.05	0.00	0.00	0.00	-0.08	0.00
Recirculation length	1.28	0.44	1.30	0.70	1.80	2.10

Table 1. Comparisons of drag and lift coefficients, and dimensionless recirculation length from ISPH and STAR-CD V4 at various Reynolds numbers (the initial particle distance dr = 0.1D for the ISPH simulations).

A good agreement between both methods is found at Re_D = 100, while some discrepancy is found at Re_D = 20. This could be due to the choice of the viscous term Eq. (12) in the SPH approach. It was showed by Issa (2005) that the viscous term proposed by Morris *et al*. (1997) provides better estimations at low Reynolds number.

Another problem resides in that the maximum bulk velocity is overestimated by ISPH. This over-prediction is explained in Issa (2005), though it might be linked to the size of the kernel support. Various tests on the choice of the kernel and of the smoothing length will be required.

The compact support shape obviously contributes to the accuracy of the method. The "physical disk" shape for particles far from a boundary degenerates in a truncated one for particles located near a boundary, if no special treatment is made for those particles. To circumventing this, normalisation of the kernel should be carried out, although it increases CPU time.

Lastly, the pressure boundary condition for solid boundaries is still a critical issue due to the nature of SPH methods. Concerning the CPU time and the accuracy of the method, robust treatments at the boundary should be studied.

REFERENCES

Chorin A.J. (1968), Numerical solution of the Navier-Stokes equations, *Math. Comp.*, 22, 745-762.

Cleary P.W. and Monaghan, J.J. (1999), Conduction modelling using Smoothed Particle Hydrodynamics. *J. Comp. Phys.*, 148, 227-264.

Cummins S.J. and Rudman M. (1999), An SPH projection method, *Journal of Computational Physics,* 152, 584-607.

Dhiman A.K., Chhabra, R.P. and Eswaran V. (2005), Flow and hear transfer across a confined square cylinder in the steady flow regime: Effect of Peclet number, *International Journal of Heat and Mass transfer,* 48, 4598-4614.

Issa R. (2005), Numerical assessment of the Smoothed Particle Hydrodynamics gridless method for incompressible flows and its extension to turbulent flows, *PhD thesis report*, *Univ. of Manchester (UK).*

Kim D.-H., Yang K.-S. and Senda M. (2004), Large eddy simulation of turbulent flow past a square cylinder confined in an channel, *Computers & Fluids,*33, 81-96.

Monaghan J.J. (1992), Smoothed Particle Hydrodynamics, *Annual Review of Astrophysics*, 30, 543-574.

Morris J.P., Fox P.J. and Zhu Y. (1997), Modelling low Reynolds number incompressible flow using SPH, *J. Comp. Phys.,* 136, 214-226.

Shao S. and Lo E.Y.M. (2003), Incompressible SPH method for simulating Newtonian and non-Newtonian flows with a free surface, *Advances in Water Resources,* 26, 787-800.

Van Der Vorst, H.A. (1992), Bi-CGSTAB: A fast and smoothly converging variant of Bi-CG for the solution of non-symmetric linear systems, *Siam J. Sci. Stat.*, 13, 631-644.